Cretaceous Research 128 (2021) 104960

Contents lists available at ScienceDirect

Cretaceous Research

journal homepage: www.elsevier.com/locate/CretRes

Short communication

Synchrotron X-ray microdiffraction to study dental structures in Cretaceous crocodylomorphs

O. Vallcorba [a], M. Canillas [b], J. Audije-Gil [c, d, *], F. Barroso-Barcenilla [d, e], A. González-Martín [c], J. Molera [f], M.A. Rodríguez [b], O. Cambra-Moo [c]

[a] ALBA Synchrotron Light Source, Cerdanyola del Vallès, Barcelona, Spain
[b] Instituto de Cerámica y Vidrio, CSIC, Madrid, Spain
[c] Laboratorio de Poblaciones del Pasado (LAPP), Departamento de Biología, Facultad de Ciencias, Universidad Autónoma de Madrid, Madrid, Spain
[d] Paleontología Ibérica (PaleoIbérica), Departamento de Geología, Geografía y Medio Ambiente, Universidad de Alcalá, Alcalá de Henares, Madrid, Spain
[e] Procesos Bióticos Mesozoicos, Departamento de Geodinámica, Estratigrafía y Paleontología, Universidad Complutense de Madrid, Madrid, Spain
[f] MECAMAT, Universitat de Vic, Universitat Central de Catalunya, Campus Torre dels Frares, Vic, Spain

ARTICLE INFO

Article history:
Received 21 July 2020
Received in revised form
8 June 2021
Accepted in revised form 11 July 2021
Available online 15 July 2021

Keywords:
Teeth
Cretaceous
Crocodylomorph
Crocodylus niloticus
Synchrotron radiation
X-ray microdiffraction
Biological apatite

ABSTRACT

Synchrotron radiation X-ray microdiffraction (SR-μXRD) has been applied for the first time as a fundamental method of analysis to unveil crocodilian teeth growth and development. Teeth from a fossil crocodylomorph from the Upper Cretaceous site of Lo Hueco (Spain) and a modern crocodylian from the living species *Crocodylus niloticus* have been analysed. Both samples have been studied through Polarized Light Microscopy, Scanning Electron Microscopy coupled with Energy Dispersive X-Ray Spectroscopy, Confocal Raman Spectroscopy, and SR-μXRD. Significant differences have been found in hydroxyapatite (HA) crystallite sizes and texture, and the evolution of these two features along teeth depth. The main differences observed in crystallite size are related to postdepositional processes and/or the environmental and functional pressures of teeth during crocodylomorph life, very different from that of the modern specimen. Regarding the crystalline texture in the tooth enamel, it can be linked to teeth functionality during crocodilian life, causing the directed growth of HA crystallites due to the mechanical stress to which they are subjected.

1. Introduction

Crocodylomorpha represents a very diverse group of reptiles that played a key role in many Mesozoic ecosystems (Densmore and Owen, 1989). Although most of the representatives of this group disappeared at the end of the Cretaceous, there are still living lineages around the world. All these living species show varied physiological patterns and different lifestyles, but their body shape and ecology have not changed much compared to those of the origin of the lineage in the Cretaceous (Densmore and Owen, 1989; Oaks, 2011; Grigg and Kirshner, 2015).

The inner anatomy of a tooth consists of three tissue typologies, enamel, dentine, and cementum (Fig. S1). It is conserved among non-fish vertebrates, regardless of the number, shape, and position of teeth in each group (Butler, 1995). As in most extinct and living vertebrates, crocodilian teeth are a biological composite where each tissue typology presents different proportions of an extracellular matrix of biological apatite and an organic component, mainly collagen fibres. The biological apatite usually appears in the form of nanometric cryptocrystalline hydroxyapatite (HA; Hurlbut and Klein, 1982). Both components can fossilize so that their spatial organization and tissue microanatomy can be analysed even in very ancient vertebrate remains (Chinsamy, 2005; Hillson, 2005).

The shape of the teeth and their microanatomy depend, among other factors, on the feeding of the animals and the phylogenetic history of the species (Dean, 2000). Crocodilian teeth are continuously shed and replaced to maintain a permanent functional dentition (Poole, 1961; Thomadakis, 2015). Teeth shape and microanatomy change during dentition formation and growth. This process leaves a record in the microstructure: alternate short and long-growth period lines can be observed along the dentine (Dean, 2000; Hillson, 2005). On the one hand, the thin and regular lines

* Corresponding author. Laboratorio de Poblaciones del Pasado (LAPP), Departamento de Biología, Facultad de Ciencias, Universidad Autónoma de Madrid, Madrid, Spain.
E-mail addresses: julia.audije@uah.es, julia.audije@estudiante.uam.es (J. Audije-Gil).

https://doi.org/10.1016/j.cretres.2021.104960

identified as short-period incremental lines, or von Ebner lines (Ebner, 1906), corresponding to the circadian rhythm of dentine deposition (Erickson, 1992, 1996; Dean, 2000). On the other hand, the wide and non-regular bands identified as long-period incremental lines, or Andresen lines (Andresen, 1898), representing long depositional periods of dentine formation (Dean, 2000). The number of days that these long-period incremental lines reflect depends on the species and the influence of the environment on the growth of each individual. In general, both short and long-period incremental lines allow inferring dentine formation rates, tooth growth, and development of extinct and extant species because they represent the record of teeth tissue formation and odontogenesis (Erickson, 1992, 1996).

Many high-resolution analytical techniques have been incorporated for the study of bones and teeth microstructure and chemical composition in recent times: *i.e.*, X-Ray Tomography, Raman Spectroscopy, Scanning Electron Microscopy coupled with Energy Dispersed Spectroscopy, and X-Ray Diffraction. However, not many results have been reported related to extinct and living crocodilian species (Dauphin and Williams, 2007, 2008; Enax et al., 2013; Wu et al., 2013; Thomadakis, 2015). In particular, only a few works apply X-Ray Diffraction (XRD) to study biomineralized fossil materials. One example is the work of Trebacz and Pikus (2003) using an experimental living model (rat bones) to propose that changes in bone structure could be related to animal activity. Also, Yamada et al. (2018) used a 1 mm diameter X-ray beam to study the residual stresses generated during bone formation and reconstruction in bovine femurs of different ages. These are experimental evidence showing that a crystallographic study of bones and teeth is useful to obtain information about biological aspects from extinct and living species. In this sense, the use of a micrometric X-ray beam opens the door to *in situ* mappings of biomineralized materials, to understand the orientation of crystallites (Nakano et al., 2002, 2009; Miyabe et al., 2007) and the structural changes (Meneghini et al., 2003).

Within this context, the main objective of this work is to study and to compare the differences between a Cretaceous crocodylomorph and a modern crocodile from the crystallographic point of view. In addition to other techniques, Synchrotron radiation X-ray microdiffraction (SR-μXRD) has been carried out for the first time as a fundamental method of analysis of biological apatite quality, maturation, and mechanical influences, involved in tooth growth and development.

2. Materials and methods

2.1. Materials

The studied samples consist of teeth cross-sections of a Cretaceous crocodylomorph and a modern crocodile. The crocodylomorph tooth, G2-W-016, belongs to a non-Crocodylia eusuchian from the Upper Cretaceous *Konzentrat-Lagerstätte* of Lo Hueco (Fuentes, Central-Eastern Spain; see the location map in Barroso-Barcenilla et al., 2009; Cambra-Moo et al., 2012). This site was discovered and excavated in 2007. It is stratigraphically located in the upper part of the Villalba de la Sierra Formation (Barroso-Barcenilla et al., 2009) and records a succession of marly mudstone levels (V, G1, R1, G2, R2, and M), some of them crossed by a sandy channel structure (C) and a sulphated interval (S). Lo Hueco represents one of the most interesting upper Campanian-lower Maastrichtian palaeontological sites for the European fossil record due to the high density of remains and diversity of taxa preserved (*i.e.*, fishes, turtles, lizards, crocodiles, dinosaurs). This outcrop is interpreted as formed in a near coastal marsh and muddy flood plain with brackish to freshwater aquatic influence. Most of its remains were rapidly buried after death and present no evidence of erosional agents. Consequently, the fossils of Lo Hueco are usually well preserved, including vegetal and vertebrate tissue microanatomy, which provide a large amount of palaeobiological information about the original organism (Cambra-Moo et al., 2012, 2013). Most of the best-preserved vertebrate remains come from the grey marly mudstone levels G1 and G2. The fossil tooth of the present study comes from the G2 level. The modern crocodilian tooth, KD6, has been studied as the living model. It belongs to an early adult stage specimen assigned to the living crocodylian African species *Crocodylus niloticus* Laurenti, 1768. This material comes from an individual bred in captivity, and it was donated by the crocodile farm Granja de Cocodrilos Kariba (Jerez de la Frontera, Southern Spain). The individual died by natural causes and was buried to full skeletonization without using any chemical product.

2.2. Methods

Both fossil and modern samples were embedded into an epoxy resin under vacuum, transversely cut with a diamond disc, ground down to 500 μm thickness, and polished with 4000 grade SiC paper. A previously prepared longitudinal thin section was observed under Polarized Light Microscopy for the description of dental histology of the fossil specimen. Then, the polished samples were characterized through Polarized Light Microscopy (PLM), Scanning Electron Microscopy coupled with Energy Dispersive X-Ray Spectroscopy (SEM-EDS), Confocal Raman Spectroscopy (Raman), and Synchrotron radiation X-ray microdiffraction (SR-μXRD). Both samples and corresponding sections are temporary held at the Departamento de Geología, Geografía y Medio Ambiente (Universidad de Alcalá, Alcalá de Henares, Madrid, Spain).

2.2.1. PLM

Teeth samples were observed using a linearly polarized light microscope (CX31, Olympus Corporation, Tokyo, Japan) and imaged at 4x magnification with a 10.0MP digital USB camera (A35100U, OMAX Corporation, Kent, USA). The software ToupView Driver 2.0 (Hangzhou ToupTek Photonics Co., Zhejiang, China) was used for measurements when necessary.

2.2.2. SEM-EDS

Samples were characterized with a cold cathode field emission scanning electron microscope FESEM S-4700 (Hitachi, Tokyo, Japan) operating at 20 kV of accelerating voltage and 12−14 mm of working distance. Samples were coated with a thin layer of Ag. Elemental analysis was obtained by Energy Dispersive X-Ray Spectroscopy (EDS) operating at 20 kV voltage, 60 s acquisition time, and 6 μm beam diameter.

2.2.3. Raman

Raman microscope ALPHA 300AR (WITec, Ulm, Germany) equipped with a Nd:YAG laser light source (532 nm) was used to analyse Raman spectra of a polished longitudinal section of the fossil tooth. Four points have been analysed in each tooth, in the apical and lateral enamel and dentine surfaces. The power used has been 10 mW, with 10 s exposure time, and the background has been adjusted to a 9th order polynomial to avoid fluorescence emission.

2.2.4. SR-μXRD

SR-μXRD was carried out at the Materials Science and Powder Diffraction (MSPD-BL04) beamline (Fauth et al., 2013) of ALBA Synchrotron. The zones of interest from the polished thin sections were measured in transmission geometry with a focused beam of 15×15 μm^2 (full width at half-maximum). The energy used was 29.2 keV ($\lambda = 0.4246$ Å) and the diffraction patterns were recorded

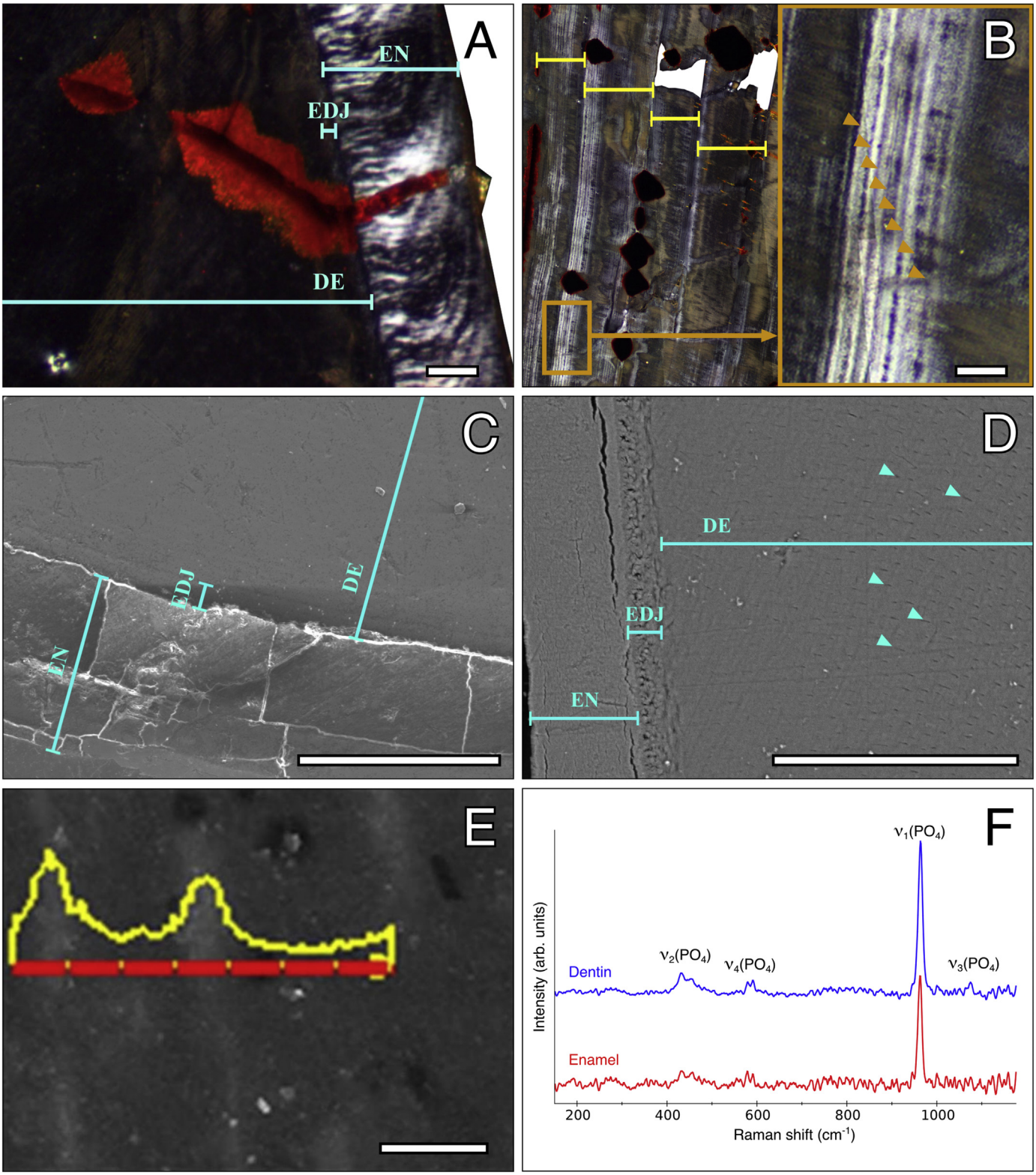

Fig. 1. Histological images under Polarized Light Microscopy (PLM) of the fossil tooth G2-W-016 (A-B), where the long (yellow lines) and short-period (orange arrowheads) incremental lines can be observed. High-resolution images by Scanning Electron Microscopy (SEM) of the fossil G2-W-016 (C) and modern KD6 (D) teeth, showing the canaliculi (blue arrowheads). Iron profile obtained from Energy Dispersive X-Ray Spectroscopy (EDS) signal on the SEM image of the fossil tooth G2-W-016 (E). Raman spectra of polished transversal section of the fossil tooth G2-W-016 (F). EN: enamel, DE: dentine, EDJ: enamel-dentine junction. Scale bars = 100 μm for A, B, D; 500 μm for C; 2.5 μm for E; 500 nm for F.

with a Rayonix SX165 CCD detector (active area of 165 mm diameter, frame size 2048 × 2048 pixels, 79 μm pixel size, dynamic range 16 bit). The calibration of the sample to detector distance and beam centre, the radial integration, azimuthal plots, and processing of the two-dimensional X-ray Diffraction (2D-XRD) images were performed with the D2Dplot software (Vallcorba and Rius, 2019). Lanthanum hexaboride (NIST 660b) data have been used for calibration and to determine the instrumental function for the microstructure analysis, which has been carried out using the spherical harmonics approximation implemented in FullProf (Rodríguez-Carvajal, 1993). For each specimen, the measurements consisted of radial line scans where a 2D-XRD pattern was collected every 10 μm along them.

3. Results

3.1. Histochemical analyses

Histological images of the polished transversal section of the fossil (G2-W-016) and modern (KD6) teeth under PLM and SEM-EDS have been obtained (Fig. 1A–D). Homogenous surfaces are observed in both specimens (Fig. 1C–D) and teeth enamel is well distinguished from dentine, with a clear interface zone between them, identified as the enamel-dentine junction (EDJ). Dentine also shows a characteristic porosity due to the presence of canaliculi (Fig. 1D), resulting from the spaces left by cytoplasmic extensions of odontocytes when dentine is deposited (Enax et al., 2013). In the fossil specimen, there are several microcracks probably originated during the fossilization processes.

SEM-EDS shows the presence of Iron (Fe) in the canaliculi and microcracks (Fig. 1E), which corresponds to the haematite phase according to the Raman spectra. In the rest of the areas, only Phosphorous (P), Calcium (Ca), and Oxygen (O) were present. Also, Raman analyses confirmed that the main phase in the fossil material corresponds to hydroxyapatite (HA; Fig. 1F), with no significant differences between different zones of the tooth.

3.2. SR-μXRD

To deeply explore the possible structural differences within the HA in each tooth, SR-μXRD measurements were carried out. A series of two-dimensional X-ray Diffraction (2D-XRD) patterns were collected every 10 μm following a 1 mm line from the surface (out of the teeth) to the dentine (Fig. 2).

The 2D-XRD patterns of the fossil sample (Fig. 3A) show well-defined Debye rings, indicating a practically random orientation of the HA crystallites in the enamel and the dentine. The integration of the rings gives rise to the corresponding powder diffraction patterns (Fig. 3B) where the only crystalline phase identified is HA.

In the case of the modern sample, the enamel diffraction patterns show intensity variations along the rings (azimuth), indicating that the spatial orientation of the HA crystallites is not random (Fig. 3C). Also in the enamel, some amorphous content is detected from a broad peak observed at 4.90° 2θ (Fig. 3D), probably coming from the embedded resin of the sample preparation, since it is not detected deeper in the teeth. As in the fossil sample, HA is the only crystalline phase identified but in this case, the diffraction peaks are broader, indicating smaller HA crystallites.

3.2.1. HA crystallite size

The evolution of the average HA crystallite size along the measured lines (towards the inside of the teeth) is detailed in Fig. 4.

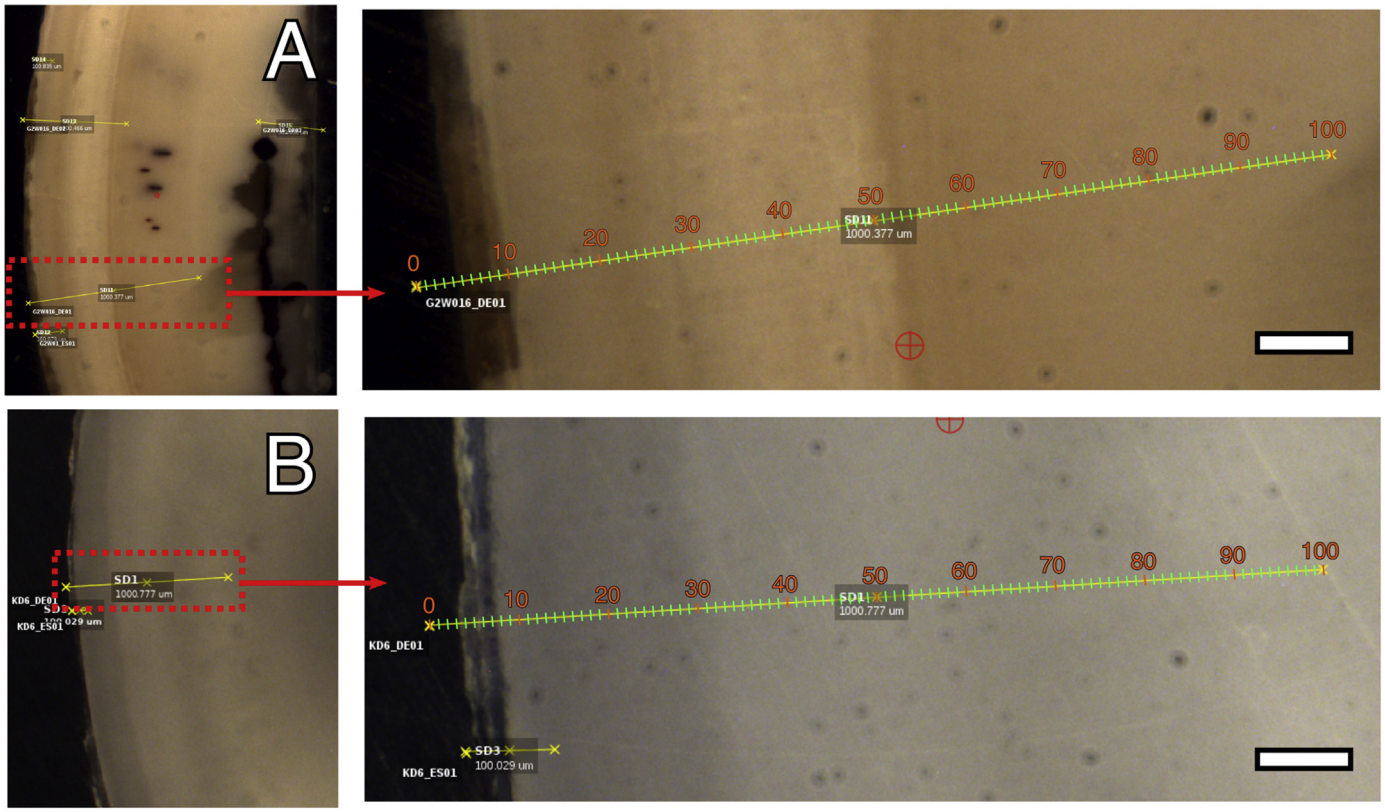

Fig. 2. Optical images of the fossil G2-W-016 (A) and the modern KD6 (B) samples analysed by Synchrotron radiation X-ray microdiffraction (SR-μXRD). Diffraction patterns were collected along the 1 mm yellow lines (one pattern every 10 μm, at the crossing green lines) from the surface to the dentine. Scale bars = 100 μm.

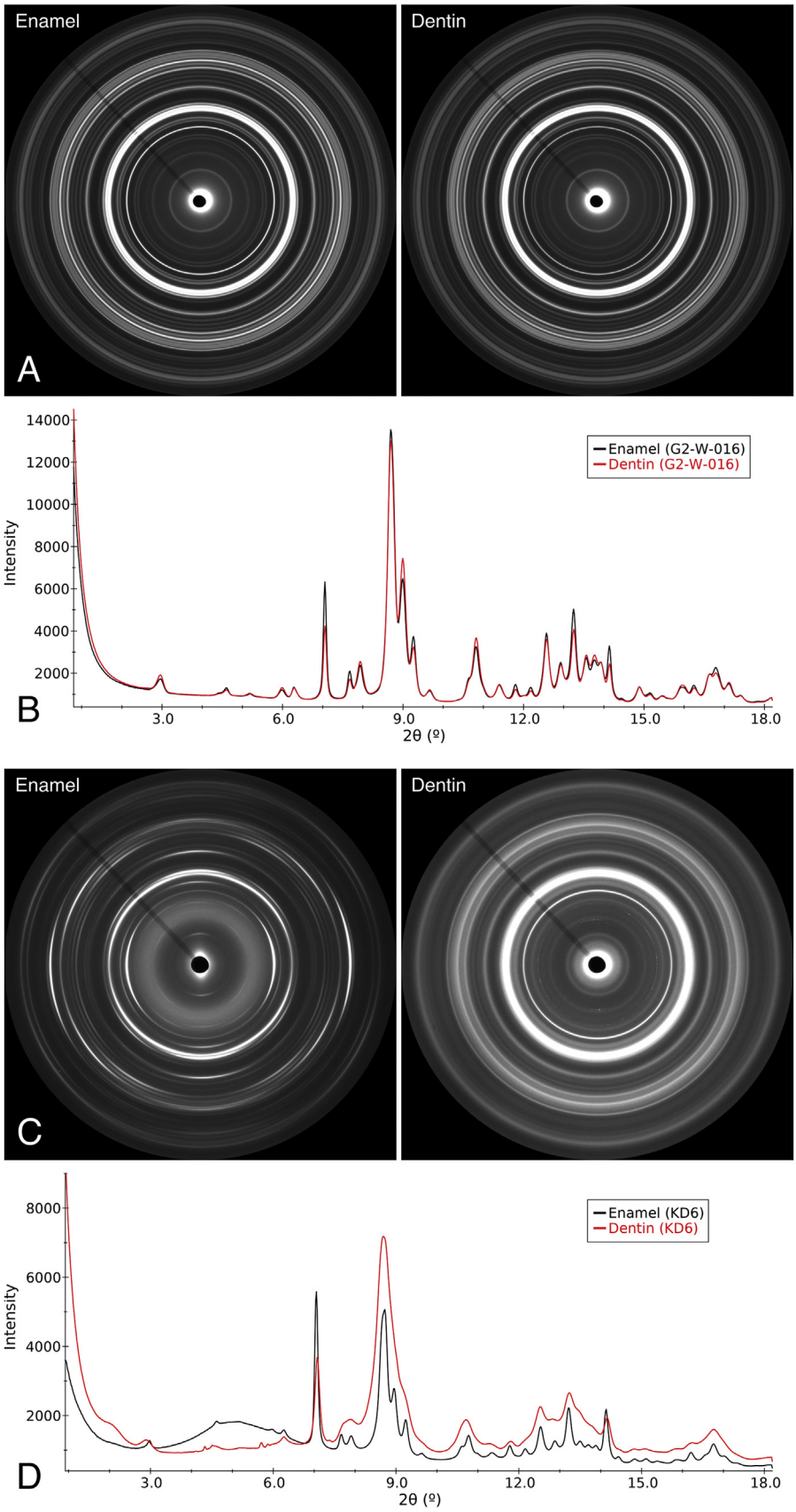

Fig. 3. Two-dimensional X-ray Diffraction (2D-XRD) patterns of the fossil tooth G2-W-016 (A), in the enamel (left) and the dentine (right). The enamel point is located at 70 μm and the dentine at 200 μm from the surface. Powder diffraction patterns obtained from the 2D-XRD data of the same tooth (B). 2D-XRD patterns of the modern tooth KD6 (C), in the enamel (left) and the dentine (right). The enamel point is located at 120 μm and the dentine at 600 μm from the surface. Powder diffraction patterns obtained from the 2D-XRD data of the same tooth (D).

It has been calculated from the peak widths obtained from the full-profile pattern matching (Figs. S2–S5). This analysis provides a semi-quantitative indication of the sample microstructure, and only the relative comparison of the values inside the same sample or between the studied teeth should be considered. The size of the crystallites in both samples shows a clear anisotropy, being longer in the *c* direction (the 00l reflections are sharper).

In the fossil specimen, the evolution of the average HA crystallite size (Fig. 4A) shows that the size in the *a*/*b* directions decreases (as a general tendency) from the enamel to the dentine, becoming constant at one point (~600 μm from the surface) where a colour change can be seen at the optical image. In contrast, the evolution of the size in the *c* direction does not show the same clear tendency and there are bigger fluctuations that match again with colour changes in the optical image.

In the modern sample, the average crystallite size in both *a*/*b* and *c* directions generally decreases with the depth, becoming almost stable after 350 μm from the surface (in the dentine; Fig. 4B). However, it is worth noting that the *c* size in the modern sample increases from the surface of the enamel to the interphase of both tissues, the EDJ, where it reaches a maximum. This result together with the behaviour of *a*/*b* directions indicates that HA crystallites tend to be less elongated and wider in the enamel, especially the ones closer to the surface, and more elongated and narrow in dentine.

3.2.2. HA crystallite orientation

Another important aspect that can be studied from the 2D-XRD images is the sample texture, in this case, the preferred orientations of the HA crystallites. Visual inspection of the diffraction images from the enamel zones shows that the distribution of the intensity along the Debye rings is not homogeneous. The intensity distribution for each reflection can be inspected by performing azimuthal plots (*i.e.*, the plot of the intensity along the Debye rings) (Fig. 5; see also Figs. S6–S7 for additional plots). The analysis of the azimuthal plot in all the 2θ range for a single image (in the enamel region, where the orientation is stronger) of the fossil and modern teeth (Fig. 5A and B, respectively) indicates a much stronger preferred orientation of the HA crystallites in the modern enamel compared to the fossil enamel. Also, the intensity distribution of the (002) and (004) reflections shows that the *c* axis of the HA crystallites in enamel is oriented perpendicular to the surface of the teeth. Taking the (002) reflection and performing its azimuthal plot at each measured point shows how deep in the teeth this orientation is preserved (Fig. 5C and D for the fossil and modern, respectively) and how it changes. In the case of the fossil, the zone where the HA is oriented is small (~75 μm from the surface) and, surprisingly, the orientation is not constant. The first layers from the surface show the same orientation as in the modern tooth (*c* axis normal to the surface) but then it changes 90° resulting in a small zone within the enamel where the *c* axis is oriented parallel to the EDJ. In the modern tooth, the orientation remains always the same and it is manifested throughout all the enamel zone, down to the dentine zone (~150-200 μm from the surface). The rest of the dentine in the modern sample shows no preferred orientation.

4. Discussion

The main crystalline phase identified in both the fossil and modern sample is hydroxyapatite (HA), as it has been confirmed by SEM-EDS, Raman, and SR-μXRD results. The analysed specimens are not closely related taxa and they cannot be directly compared. However, from the

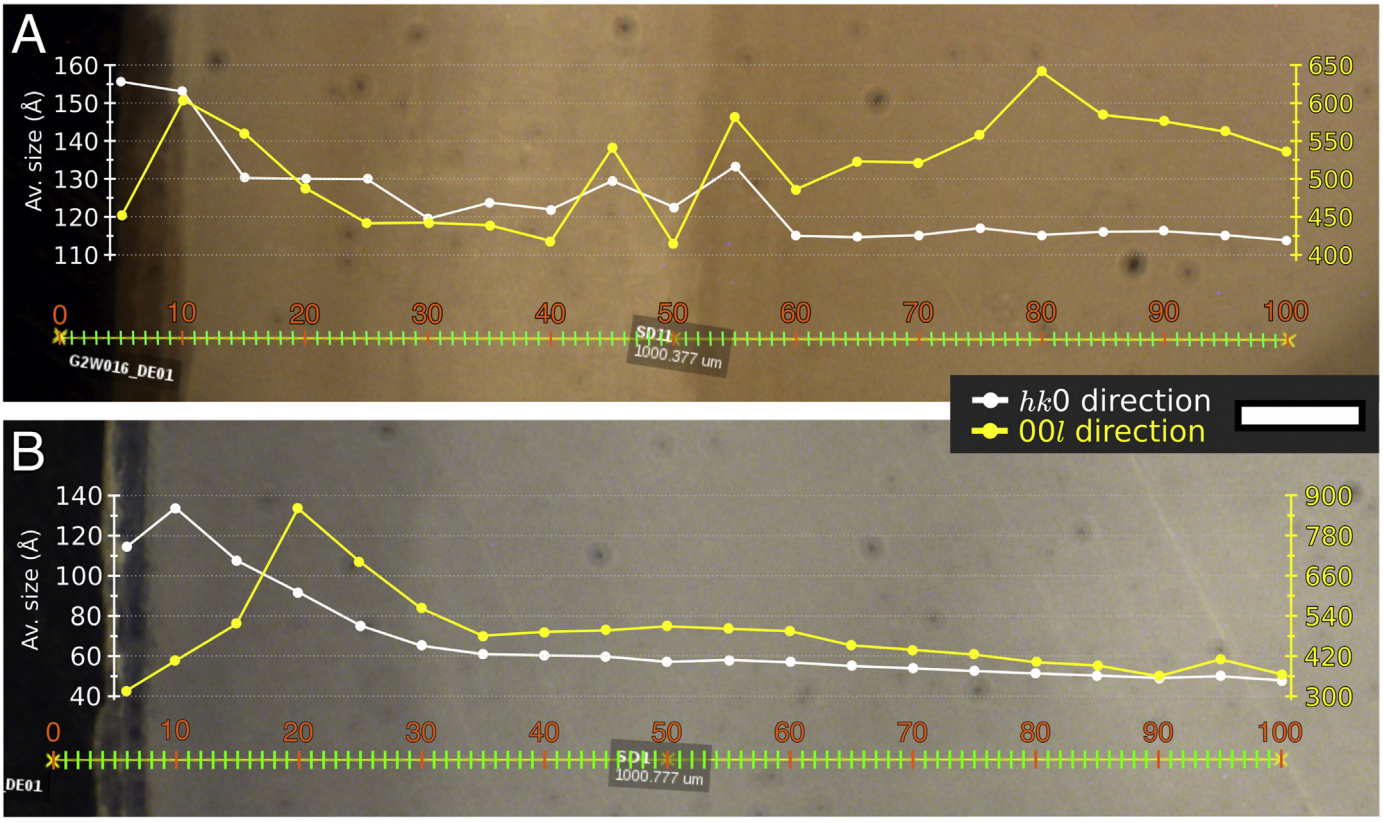

Fig. 4. Evolution of the hydroxyapatite average crystallite size in the *a*/*b* (*hk*0) and *c* (00*l*) directions with the teeth depth, for the fossil G2-W-016 (A) and the modern KD6 (B) teeth. Av: Average. Scale bar = 100 μm.

crystallographic point of view, there are some aspects worth mentioning that could be related to biological or environmental influences in the pace of life of each specimen. In this sense, there are significant differences between them regarding the coherent domain size of the HA crystallites, their preferred orientation (*i.e.*, texture), and the evolution of these two features along teeth depth.

The size of the crystallites in both samples shows a clear anisotropy by being longer in the *c* direction (the 00l reflections are sharper), which is a well-known feature of biological apatite in bones (Meneghini et al., 2003; Hillson, 2005) related with the HA hexagonal crystal shape. A first difference that can be observed between the fossil and modern specimens is the different evolution of the HA crystallite size through teeth depth, especially in the *c* direction (Fig. 4). The fossil specimen shows strong oscillations in the crystallite size, while in the modern specimen the size evolution follows a regular decreasing tendency. Crocodiles are animals with great dependence on the environment for their growth. As in other ectotherms, their development depends on daily or seasonal trends (Hutton, 1986; Castanet et al., 1988) and can be related to light, temperature, humidity, and food supply conditions (Cott, 1961; Blake and Loveridge, 1975; Revol, 1995). Therefore, the crystallite size of the HA deposited during odontogenesis may depend on how favourable or unfavourable the environmental conditions are. If this hypothesis is true, the *c* direction in HA crystallites is more regular in the modern sample because the individual was bred in captivity, in a farm where environmental conditions are controlled for the welfare of the animal (heating system, constant care, and food supply). On the contrary, the variations of the crystallite size in the fossil specimen may represent cycles related to changes in the environment, which could affect its metabolism. Moreover, the observed crystallite size fluctuations in the fossil sample (Fig. 4A) match with colour changes in the optical image. These colouration changes correspond to the wide and non-regular bands identified as long-period incremental lines that may represent periods of dentine formation where changes in the HA crystallites directions and/or collagen fibres trajectories occur (Erickson, 1996; Hillson, 2005). In the case of

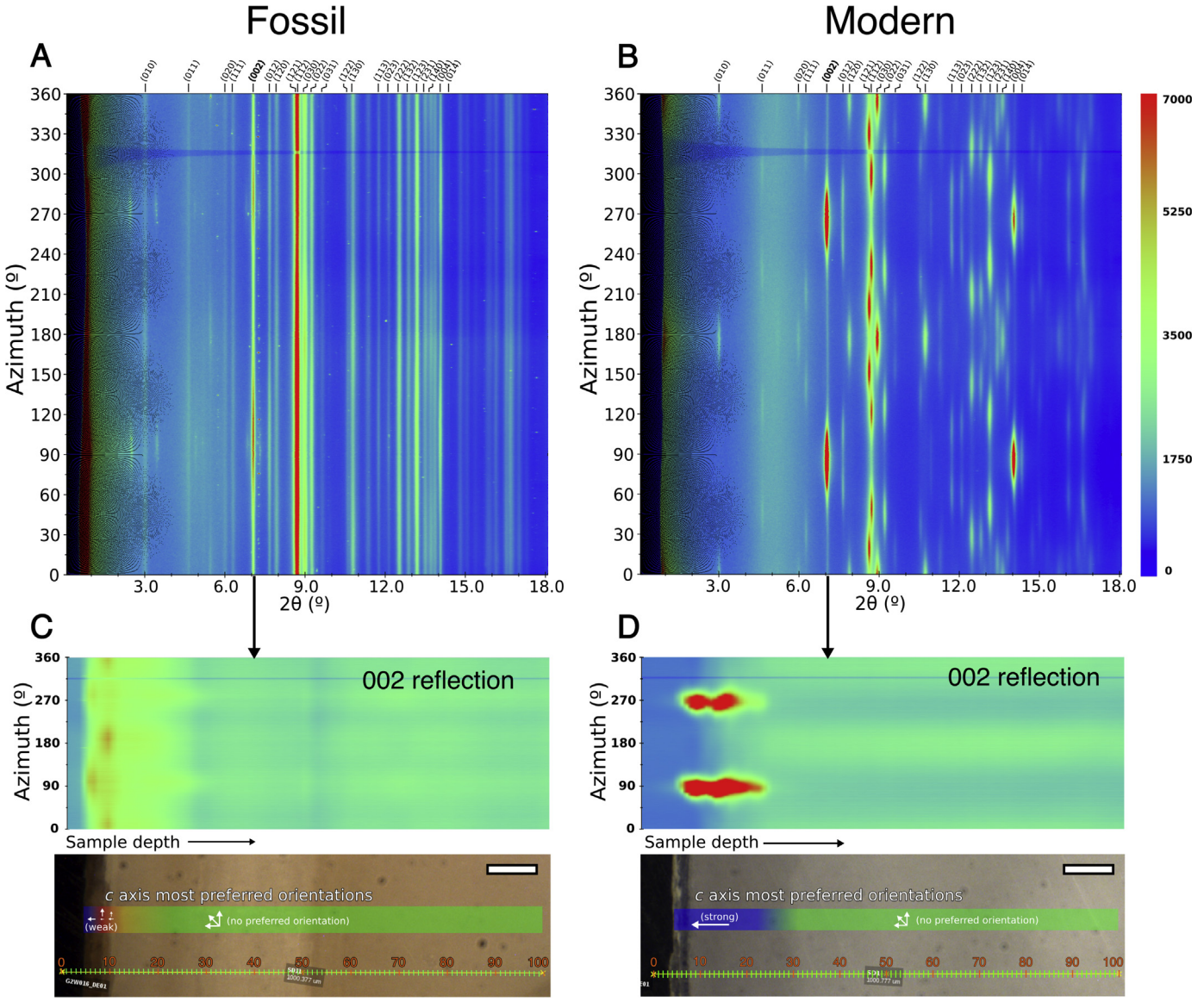

Fig. 5. Azimuthal plots from two-dimensional X-ray Diffraction (2D-XRD) for a single enamel point of the fossil G2-W-016 (A) and the modern KD6 (B) teeth. The hkl indices of the reflections are written on the top of each plot and the colour scale corresponds to the reflection intensities (detector counts). Stacking of azimuthal plots for the (002) reflection at each measured point of the same fossil (C) and modern (D) samples. Relative intensity at the same colour scale as the above plots. The preferred orientations of the *c* axis direction of the hydroxyapatite crystal structure for both teeth are represented on the respective images. Scale bar = 100 μm.

specimens from archaeological or palaeontological origin, colouration changes could be also associated with taphonomical alteration, such as adsorption of elements of the medium or secondary mineral deposition (Hillson, 2005; Gren and Lindgren, 2014). In any case, this preferential acquisition of taphonomical artefacts could be related to those intrinsic mineralization characteristics of the tissue (*i.e.*, orientation and size of the HA crystallites and/or disposition of the cellular component). In the results of the present work, long-period incremental bands in the fossil specimen seem to coincide with changes in the size of HA crystallites. This size variation is not abrupt on average and it seems to be greater between different bands than within the same long-depositional band. However, the influence of taphonomic processes on the observed crystallographic changes should not be dismissed (Carlson, 1989), since diagenesis could affect the size of the HA crystallites (Grupe, 2018), as discussed below.

The second difference that can be observed between the fossil and modern teeth is the average HA crystallite size. While HA is nanometric in both cases, in the modern specimen the crystallites are considerably smaller than in the fossil crocodylomorph. One possible cause is the pace of life of the individual. Modern tooth belongs to an individual in the young or early adult stage (Audije-Gil et al., in press) which, together with continuous replacement of teeth in crocodiles, could imply that the dental tissue in this specimen is not completely mature. In this sense, immature or faster-growing individuals (as crocodiles bred in captivity; Cott, 1961) could deposit crystals of a smaller size. The differences in crystallite size can also be caused by diagenetic processes. Crystal growth is a common alteration (Sakae et al., 1997; Hillson, 2005) since the degradation of organic material and/or the relatively high temperatures can favour this process (Grupe, 2018).

Another aspect that can be highlighted is that, in both specimens, the enamel has a larger crystallite size than the dentine. This has been already described in previous works (Carlson, 1989). In general, after the enamel deposition, this tissue undergoes a maturation process that increases its hardness and density. During this process, the size of the crystallites increases together with the decrease in the organic matter of enamel, until it becomes acellular (Sander, 2000). However, the difference between sizes in crocodiles is not as abrupt as in mammals, and the crystallite sizes in enamel and dentine are comparable (Enax et al., 2013). In general, crocodilian enamel seems to be thinner and less crystalline than in mammals, which may be related to the fact that crocodiles do not use their teeth to dismember their prey, but to capture and drown them (Grigg and Kirshner, 2015).

Regarding the preferred orientation of the HA crystallites, it is manifested only in the enamel region of both samples and it is much stronger in the modern specimen (Fig. 5). The intensity distribution of the (002) and (004) reflections shows that the *c* axis of the HA crystallites is oriented perpendicular to the surface of the tooth in the modern sample and the first layers of the fossil. This has been observed in other living crocodilian species (Enax et al., 2013) and it is classified as parallel crystallite enamel (Sander, 2000), which is perpendicular to the EDJ. Although most reptiles show this general parallel crystallite enamel pattern, many groups have shown a wide range of variability (Carlson, 1989). The arrangement of these crystallites in the fossil sample occurs in volumes or sections of enamel, known as modules. These modules have similar intrinsic characteristics (orientation, size) and are delimited by discontinuities (Sander, 2000). Two discontinuities have been observed in fossil enamel (Fig. 5C). In the first module (section separated by discontinuity), the enamel is arranged as parallel crystallite. Then crystallite orientation changes into two different modules. Although HA crystallite orientation is subjected to direct genetic control, their functional significance cannot be dismissed. So these changes observed in the fossil sample, far from having only phylogenetic constraints, could be related to functional implications (*i.e.*, to feeding habits; Sander, 2000) and, in any case, further research must be carried out to better understand these changes.

5. Conclusions

The present work represents the first study of crocodilian dental structures by Synchrotron radiation X-ray microdiffraction (SR-μXRD). Thin sections of a Cretaceous crocodylomorph and a modern *Crocodylus niloticus* have been analysed. Interpretations based on scarce material must be prudent, but they can provide valuable information considering that the microstructure and the crystallographic features of crocodilian dental tissues are poorly understood. The main crystalline phase identified in both fossil and modern specimens is hydroxyapatite (HA). The presence of the haematite phase has been only detected in canaliculi and microcracks of the fossil sample.

While the HA crystallites are nanometric in both samples, in the modern specimen their size is considerably smaller than in the fossil sample. This may be due to two non-exclusive causes. First, to the degree of maturity of the considered specimen and therefore, the lower crystalline deposition in immature specimens. Second, to diagenetic alterations, as the disappearance of organic material and/or the relatively high temperatures favours crystal growth by crystallite authigenesis and recrystallization. The crystallite size of the HA deposited during odontogenesis may also depend on how favourable or unfavourable the environmental conditions are. In this sense, long-period incremental bands in the fossil specimen seem to coincide with changes in the size of HA crystallites. Thus, variations in crystallite size may represent cycles related to individual metabolism and the influence of changes in the environment.

Concerning HA texture, both samples show that there is a preferred orientation in the enamel zone, much stronger in the case of the modern tooth, while the orientation seems to be almost random in the dentine. This fact could be linked to teeth functionality during crocodilian life, which made the HA crystallites grow directed by the mechanical stress to which they were subjected. However, the influence of taphonomic processes on the observed variations must be also considered.

Acknowledgements

These experiments were performed at the BL04 Materials Science and Powder Diffraction (MSPD) beamline of the ALBA Synchrotron (Cerdanyola del Vallès, Barcelona, Spain; proposal 2019023466). In this sense, J. Audije-Gil and O. Cambra-Moo appreciate the ease of working with ALBA facility staff. The authors also thank Á. Conde Alonso, director of the Granja de Cocodrilos Kariba (Jerez de la Frontera, Spain), for the kindly donation of the modern *Crocodylus niloticus* material for this study. We also wish to thank the two anonymous reviewers and the journal editor for all their feedback, comments, and suggestions that allowed improving substantially the original manuscript. This work was funded by the projects PGC2018-099405-B-100 (Ministerio de Ciencia, Innovación y Universidades); HAR2017-82755-P, HAR2016-78036-P, HAR2016-74846-P, HAR2017-83004-P, CGL2015-66604, CGL2015-68363 and MAT2015-67593-P (Ministerio de Economía y Competitividad, Spain); and 201860E127 (CSIC).

References

Andresen, V., 1898. Die querstreifung des dentines. Deutsche Monatsschrift für Zahnheilkunde 38, 386–389.

Audije-Gil, J., Barroso-Barcenilla, F., Cambra-Moo, O., in press. Mapping histovariability and growth patterns of Crocodylus niloticus bred in captivity and its paleobiological implications. In: Farlow, J.O., Woodward, H.N. (Eds.),

Crocodylian Biology and Archosaur Paleobiology: Studies in Honor of Ruth M. Elsey.. Indiana University Press, Bloomington.
Barroso-Barcenilla, F., Cambra-Moo, O., Escaso, F., Ortega, F., Pascual, A., Pérez-García, A., Rodríguez-Lázaro, J., Sanz, J.L., Segura, M., Torices, A., 2009. New and exceptional discovery in the Upper Cretaceous of the Iberian Peninsula: the palaeontological site of "Lo Hueco", Cuenca, Spain. Cretaceous Research 30 (5), 1268–1278.
Blake, D.K., Loveridge, J.P., 1975. The role of commercial crocodile farming in crocodile conservation. Biological Conservation 8 (4), 261–272.
Butler, P.M., 1995. Ontogenetic aspects of dental evolution. International Journal of Developmental Biology 39 (1), 25–34.
Cambra-Moo, O., Barroso-Barcenilla, F., Berreteaga, A., Carenas, B., Coruña, F., Domingo, L., Domingo, M.S., Elvira, A., Escaso, F., Ortega, F., Pérez-García, A., Peyrot, D., Sanz, J.L., Segura, M., Sopelana, A., Torices, A., 2012. Preliminary taphonomic approach to "Lo Hueco" palaeontological site (Upper Cretaceous, Cuenca, Spain). Geobios 45 (2), 157–166.
Cambra-Moo, O., Barroso-Barcenilla, F., Coruña, F., Postigo-Mijarra, J.M., 2013. Exceptionally well-preserved vegetal remains from the Upper Cretaceous of 'Lo Hueco', Cuenca, Spain. Lethaia 46 (1), 127–140.
Carlson, S.J., 1989. Vertebrate dental structures. In: Carter, J.G. (Ed.), Skeletal Biomineralization: Patterns, Processes and Evolutionary Trends. American Geophysical Union, Washington D. C., pp. 471–530
Castanet, J., Newman, D.G., Girons, H.S., 1988. Skeletochronological data on the growth, age, and population structure of the tuatara, *Sphenodon punctatus*, on Stephens and Lady Alice Islands, New Zealand. Herpetologica 4, 25–37.
Chinsamy-Turan, A., 2005. The microstructure of dinosaur bone: deciphering biology with fine-scale techniques. Johns Hopkins University Press, Baltimore.
Cott, H.B., 1961. Scientific results of an inquiry into the ecology and economic status of the Nile crocodile (*Crocodilus niloticus*) in Uganda and Northern Rhodesia. The transactions of the Zoological Society of London 29 (4), 211–356.
Dauphin, Y., Williams, C.T., 2007. The chemical compositions of dentine and enamel from recent reptile and mammal teeth—variability in the diagenetic changes of fossil teeth. CrystEngComm 9 (12), 1252–1261.
Dauphin, Y., Williams, C.T., 2008. Chemical composition of enamel and dentine in modern reptile teeth. Mineralogical Magazine 72 (1), 247–250.
Dean, M.C., 2000. Incremental markings in enamel and dentine: what they can tell us about the way teeth grow. In: Teaford, M.F., Smith, M.M., Ferguson, M.W. (Eds.), Development, function and evolution of teeth. Cambridge University Press, Cambridge, pp. 119–130.
Densmore III, L.D., Owen, R.D., 1989. Molecular systematics of the order Crocodilia. American Zoologist 29 (3), 831–841.
von Ebner, V., 1906. Über die Entwicklung der leimgebenden Fibrillen, insbesondere im Zahnbein. Sitzungsberichte der Mathematisch-Naturwissenschaftlichen Klasse der kaiserlichen Akademie der Wissenschaften in Wien 115, 281–347.
Enax, J., Fabritius, H.O., Rack, A., Prymak, O., Raabe, D., Epple, M., 2013. Characterization of crocodile teeth: correlation of composition, microstructure, and hardness. Journal of Structural Biology 184 (2), 155–163.
Erickson, G.M., 1992. Verification of von Ebner incremental lines in extant and fossil archosaur dentine and tooth replacement rate assessment using counts of von Ebner lines (PhD thesis). Montana State University, p. 54.
Erickson, G.M., 1996. Daily deposition of dentine in juvenile Alligator and assessment of tooth replacement rates using incremental line counts. Journal of Morphology 228 (2), 189–194.
Fauth, F., Peral, I., Popescu, C., Knapp, M., 2013. The new material science powder diffraction beamline at ALBA synchrotron. Powder Diffraction 28 (S2), S360–S370.
Gren, J.A., Lindgren, J., 2014. Dental histology of mosasaurs and a marine crocodylian from the Campanian (Upper Cretaceous) of southern Sweden: incremental growth lines and dentine formation rates. Geological Magazine 151 (1), 134–143.
Grigg, G., Kirshner, D., 2015. Biology and evolution of crocodylians. Cornell University Press, Ithaca.
Grupe, G., 2018. Taphonomy and fossilization. The International Encyclopedia of Biological Anthropology 1–8.
Hillson, S., 2005. Teeth. Cambridge University Press, Cambridge.
Hurlbut, C.S., Klein, C., 1982. Manual de mineralogía de Dana. Editorial Reverté, Barcelona.
Hutton, J.M., 1986. Age determination of living Nile crocodiles from the cortical stratification of bone. Copeia 2, 332–341.
Laurenti, J.N., 1768. Specimen medicum, exhibens synopsin reptilium emendatam cum experimentis circa venena et antidota reptilium austracorum, quod authoritate et consensu. Joan Thomae, Vienna.
Meneghini, C., Dalconi, M.C., Nuzzo, S., Mobilio, S., Wenk, R.H., 2003. Rietveld refinement on X-Ray diffraction patterns of bioapatite in human fetal bones. Biophysical Journal 84 (3), 2021–2029.
Miyabe, S., Nakano, T., Ishimoto, T., Takano, N., Adachi, T., Iwaki, H., Kobayashi, A., Takaoka, K., Umakoshi, Y., 2007. Two-dimensional quantitative analysis of preferential alignment of BAp c-axis for isolated human trabecular bone using microbeam X-ray diffractometer with a transmission optical system. Materials transactions 48 (3), 343–347.
Nakano, T., Kaibara, K., Tabata, Y., Nagata, N., Enomoto, S., Marukawa, E., Umakoshi, Y., 2002. Unique alignment and texture of biological apatite crystallites in typical calcified tissues analyzed by microbeam X-ray diffractometer system. Bone 31 (4), 479–487.
Nakano, T., Fujitani, W., Ishimoto, T., Umakoshi, Y., 2009. Adaptation of BAp crystal orientation to stress distribution in rat mandible during bone growth. Journal of Physics: Conference Series 165 (1), 012084.
Oaks, J.R., 2011. A time-calibrated species tree of Crocodylia reveals a recent radiation of the true crocodiles. Evolution: International Journal of Organic Evolution 65 (11), 3285–3297.
Poole, D.F.G., 1961. Notes on tooth replacement in the Nile crocodile *Crocodilus niloticus*. Proceedings of the Zoological Society of London 136 (1), 131–140.
Revol, B., 1995. Crocodile farming and conservation, the example of Zimbabwe. Biodiversity and Conservation 4 (3), 299–305.
Rodríguez-Carvajal, J., 1993. Recent advances in magnetic structure determination by neutron powder diffraction. Physica B 192 (1–2), 55–69.
Sakae, T., Suzuki, K., Kozawa, Y., 1997. A short review of studies on chemical and physical properties of enamel crystallites. Tooth Enamel Microstructure, Balkema, Rotterdam, pp. 31–39.
Sander, P.M., 2000. Prismless enamel in amniotes: terminology, function, and evolution. In: Teaford, M.F., Smith, M.M., Ferguson, M.W. (Eds.), Development, function and evolution of teeth. Cambridge University Press, Cambridge, pp. 92–106.
Thomadakis, C., 2015. The mechanisms of continuous tooth replacement in the Nile crocodile (*Crocodylus niloticus*) (PhD thesis). University of the Witwatersrand, p. 235.
Trebacz, H., Pikus, S., 2003. A study of mineral phase in immobilized rat femur: structure refinements by Rietveld analysis. Journal of Bone and Mineral Metabolism 21 (2), 80–85.
Vallcorba, O., Rius, J., 2019. d2Dplot: 2D X-ray diffraction data processing and analysis for through-the-substrate microdiffraction. Journal of Applied Crystallography 52 (2), 478–484.
Wu, P., Wu, X., Jiang, T.X., Elsey, R.M., Temple, B.L., Divers, S.J., Glenn, T.C., Yuan, K., Chen, M.H., Widelitz, R.B., Chuong, C.M., 2013. Specialized stem cell niche enables repetitive renewal of alligator teeth. Proceedings of the National Academy of Sciences of the United States of America 110 (22), E2009–E2018.
Yamada, S., Onuma, M., Todoh, M., Tadano, S., 2018. Changes of residual stress, diaphyseal size, and micro-nano structure in bovine femurs during growth and maturation. Journal of Biomechanical Science and Engineering 13 (3), 18–110.

Appendix A. Supplementary data

Supplementary data to this article can be found online at https://doi.org/10.1016/j.cretres.2021.104960.